Light Emitting Micropatterns of Porous Si Created at Surface Defects

P. Schmuki,[1] L. E. Erickson,[2] and D. J. Lockwood[2]
[1]*Swiss Federal Institute of Technology (ETH/EPFL), Department of Materials Science, LC-DMX, CH-1015 Lausanne, Switzerland*
[2]*Institute for Microstructural Sciences, National Research Council of Canada (NRC), Ottawa, Ontario, Canada K1A 0R6*
(Received 12 January 1998)

We report a principle that allows one to write visible light emitting silicon patterns of arbitrary shape down to the submicrometer scale. We demonstrate that porous Si growth can electrochemically be initiated preferentially at surface defects created in an n-type Si substrate by Si^{++} focused ion beam bombardment. For n-type material in the dark, the electrochemical pore formation potential (Schottky barrier breakdown voltage) is significantly lower at the implanted locations than for an unimplanted surface. This difference in the threshold voltages is exploited to achieve the selectivity of the pore formation process. [S0031-9007(98)05935-3]

PACS numbers: 78.55.Ap, 61.72.–y, 81.40.Tv, 82.45.+z

Silicon is currently the technologically most important semiconductor material. However, applications in semiconductor photonics seemed unlikely due to its indirect electronic band gap [1]. Therefore, the discovery of electrochemically formed visible light emitting porous Si [2–4] has, in the past few years, stimulated intense and still-increasing research activity (see, e.g., Refs. [5–8]). The main reason for this tremendous interest is the prospect of light emitting devices made of porous Si [1,9].

Prior approaches to producing porous Si patterns mostly use photolithographic techniques [10]. An interesting alternative direct patterning process [11] uses light-induced carrier generation in n-type material under anodic electrochemical bias, which allows a selective pore formation in illuminated areas of a Si wafer. However, since direct writing approaches are generally sized limited by the diffraction limit of the light source, we used high energy ion implantation for pattern definition.

In contrast to previous ion beam work [10,12–15], we used Si^{++} as the implanting species to avoid any doping effects of the implantation and at a sufficiently high energy to minimize surface sputtering effects. From an Au-Si liquid metal ion source, Si^{++} ions were selected at 200 keV using an $\mathbf{E} \times \mathbf{B}$ mass filter and implanted in n-type Si (100) wafers (doped with 5×10^{15} cm^{-3} As) at room temperature using a 100 kV JEOL 104 UHV FIB system with a nominal beamwidth of 100 nm. By vector scanning the ion beam, different patterns (squares, lines, letters, dots) were implanted. Each pattern was implanted with dosages of 3×10^{13}, 10^{14}, 3×10^{14}, 10^{15}, 3×10^{15}, 10^{16}, and 3×10^{16} ions cm^{-2}. For doses greater than 10^{15} cm^{-2}, the implanted features can be faintly detected with a scanning electron microscope (SEM), which can be attributed to amorphization of the substrate occurring at higher implantation doses [15] or to defect-induced surface bulging [16].

The number and distribution of defects created by the implantation as well as of the sputter yield were estimated by calculations using TRIM code [17]. The vacancy depth-profile calculation shows that the creation of vacancies occurs immediately below the surface, and peaks at 270 nm below the surface. About 1500 unrecombined vacancy/interstitial pairs are formed for one incoming ion and a sputter yield of less than 0.2 is obtained. Hence the calculations show that surface sputter effects can be neglected, and that most defect creation occurs in a near surface region of the Si substrate.

The implanted samples were then electrochemically treated in 20% HF by stepping the voltage (potential) from -0.5 V to different anodic potentials with a rate of 10 mV every 5 s. In contrast to conventional porous Si formation on n-type material, the electrochemical treatment was always performed in the dark to avoid light-induced carrier generation in the semiconductor sample. Under these conditions (similar to the diode behavior of a p/n junction under reverse bias), the holes (h^+) necessary for Si^0 oxidation and dissolution as $(SiF_6)^{2-}$ become only sufficiently available at the Si surface at potentials where Schottky barrier breakdown occurs [18,19].

Figure 1 shows a typical current/voltage characteristic for a reference (nonimplanted) n-type Si sample in 20% HF. Starting from the open circuit potential, with an increasing voltage (potential) the current increases up to a plateau region. In this region, the current is controlled by electrons that overcome the charge carrier depletion region (Schottky barrier) at the semiconductor/electrolyte interface by thermal activation.

At a potential of approximately 3.8 V versus the saturated calomel electrode (SCE), the current steeply increases. In this region, local dissolution processes occur on the Si surface which, after extended polarization, lead to a porous surface. Hence this potential is called the pore formation potential (PFP). There are a variety of factors that influence the PFP such as the concentration of the anion in the electrolyte or the temperature. The predominant factors are, however, the conduction type and doping concentration of the substrate [20], as expected from the Schottky approach. In addition, the defects created by the focused

 0031-9007/98/80(18)/4060(4)$15.00

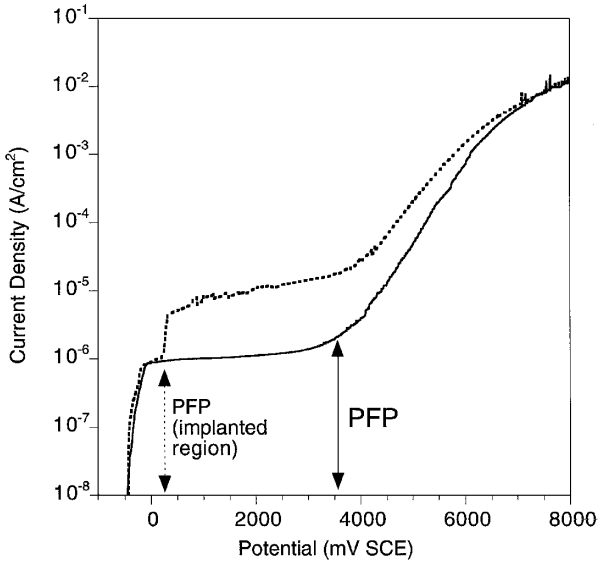

FIG. 1. Current-voltage (polarization) curve of n-type Si (100) ($N_d = 5 \times 10^{15}$ cm^{-3}) in 20% HF (solid line) and the polarization curve acquired with a $\phi = 300$ μm capillary electrode on a 50×50 μm square implanted with 3×10^{14} cm^{-2} Si^{++} (dashed line). The curves were acquired in the dark. The potentials are referred to the saturated calomel electrode (SCE).

ion beam (FIB) also have a drastic effect on the PFP. This is clear from the second curve included in Fig. 1 which shows a polarization curve acquired with a microelectrode pipette ($\phi = 300$ μm) that was placed on a 50×50 μm implanted square (dose $= 3 \times 10^{14}$ cm^{-2}). In this case, a first significant current increase appears at +0.25 V SCE. Although the implanted area is only about 3% of the total area exposed to the electrolyte, the current density in the plateau region is more than a decade higher than for the reference sample. Hence, the effective current density in the implanted region is about 300 times higher than on the intact Si surface; i.e., it becomes comparable to current densities observed with the reference sample above the PFP. If the voltage scan with implanted samples is stopped at 3.5 V, i.e., below the overall PFP, then a surface morphology as shown in the micrographs of Figs. 2 and 3 is obtained. Figure 2 shows an optical micrograph for a sample where letters were written with the FIB at a dose of 3×10^{14} cm^{-2}. The letters show the typical porous Si interference colors ranging from red to green. The letter R was obtained with a single FIB scan which results in a linewidth of approximately 300 nm. Figure 3(a) shows a SEM micrograph of a square implanted with the same dose (3×10^{14} cm^{-2}) and identically treated. From Fig. 3(b), it is apparent that porous Si has been formed within the square. The surrounding area is completely unattacked.

The photoluminescence (PL) spectrum in Fig. 4 was measured with an argon laser beam focused in the center of the 50 μm square of Fig. 3. The PL spectrum peaks at 655 nm in the orange-red region of the spectrum and,

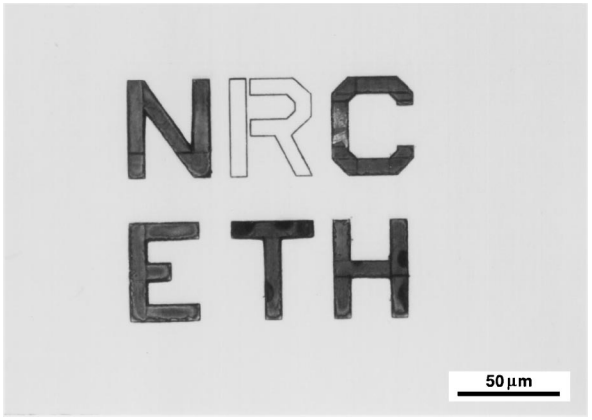

FIG. 2. Optical micrograph of porous Si letters produced by Si^{++} FIB implantation in n-type Si (100) and subsequent electrochemical polarization in 20% HF from −0.5 V SCE to 3.5 V SCE. The dose of the implant is 3×10^{14} cm^{-2}. The R in NRC was outlined with a single (100 nm) FIB line; the rest of the letters were uniformly implanted. The letters show the green and red interference colors typical of porous Si.

in width and wavelength position, is typical of the PL response of porous Si. The band shape shows irregularities that can be attributed to nanoscopic nonuniformities in the material porosity. Electrochemically treated areas next

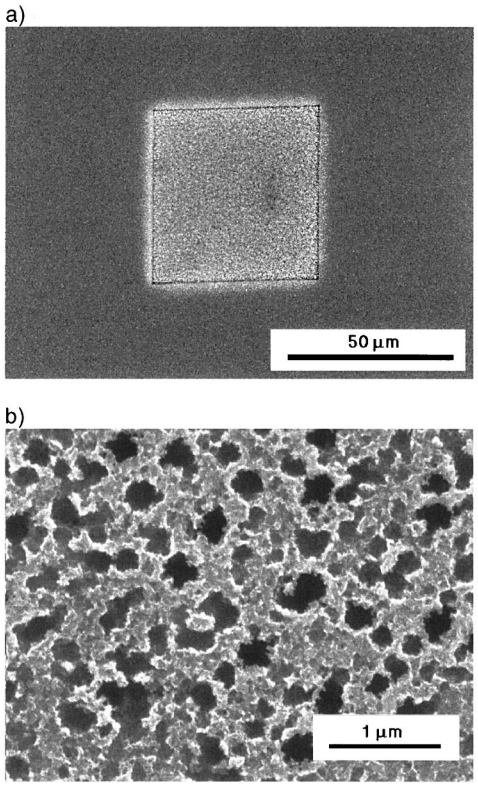

FIG. 3. (a) SEM image of a 50×50 μm square implanted with 3×10^{14} cm^{-2} Si^{++} after polarization in 20% HF from −0.5 to 3.5 V. (b) Higher magnification of (a) within the square.

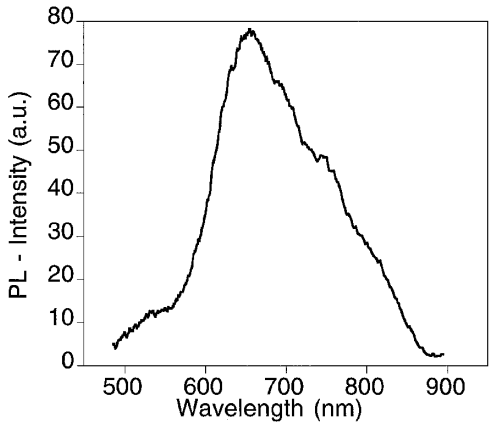

FIG. 4. Room temperature photoluminescence spectrum acquired in the center of the square shown in Fig. 3. The spectrum was excited using 15 mW of 457.9 nm argon laser light, dispersed with a Spex 14018 double spectrometer, and detected with a cooled RCA 31034A GaAs photomultiplier.

to the implanted patterns were investigated as a reference and, in every case, the unimplanted areas showed the spectral behavior of a clean Si surface (no light emission in the visible range) as did implanted areas not yet electrochemically treated. This clearly indicates that the electrochemical formation of porous Si is responsible for the PL observed and not lattice defects or amorphization created by the implantation.

It is thus clear that, at the FIB created defects, pore growth can be triggered at voltages significantly lower than at the intact area. This can be attributed to Schottky barrier breakdown, which is facilitated at defects due to an inhomogeneous field distribution at a defect site. In other words, in the potential range between the PFP of the implanted area (+0.25 V) and the PFP of the untreated area (+3.8 V), pores can be selectively formed at ion beam treated parts of the sample. This is in complete contrast with earlier ion implantation work, where the usual electrochemical treatment using constant current and p-type material, or n-type material under illumination, resulted in porous Si formation only in unimplanted regions [10,15]. This discrepancy must be associated to the different experimental conditions, i.e., the use of n-type material in the dark in the present work which makes Schottky barrier breakdown the determining criterion for h^+ availability at the sample surface and thus for dissolution.

With a set of samples, polarization experiments were performed by acquiring a polarization curve from −0.5 to 1, 2, 3.5, and 5 V. For all voltages and for all investigated implantation doses, selective dissolution or etching was observed. As expected for the sample that was exposed to 5 V (i.e., anodic to the overall PFP), etching was not confined to the implanted areas but spread over the entire surface. The rest of the samples showed that the morphology of the selective attack depends strongly on the implantation dose and on the electrochemical treatment. Samples implanted with doses greater than 10^{15} cm^{-2} and treated up to 3.5 V showed a selective etching of the entire implanted area rather than pore formation. For samples implanted with a dose of less than 10^{14} cm^{-2} and treated to 1 V, pore formation was not uniform and only some porous patches were formed within the implanted area.

The highest PL intensity was observed from the sample implanted with a dose of 3×10^{14} cm^{-2} and polarized to 3.5 V (Fig. 4). Other conditions led to significantly lower PL intensities. PL intensity and morphology of the samples correlate in that, for the highest PL sample, the highest amount of porosity with feature sizes in the nanoscopic range was found, which is consistent with a quantum confinement explanation for the red PL of porous Si [20].

It is noteworthy that, not only for lines and single line letters (as in Fig. 2) but also for circular shapes, the local dissolution process occurred at the implantation and did not follow the crystal orientations of the bulk Si, i.e., no branching out of the etch was observed along undamaged crystalline Si planes, and that the etching stopped when the underlying undamaged crystalline Si was reached. Thus, this indicates that the reaction activation energy at defects is much lower than for crystal planes exposed during the dissolution.

In summary, we have shown how to produce laterally confined light emitting Si by a direct writing process. We clearly demonstrate that a creation of surface defects followed by an electrochemical treatment, tailored to trigger dissolution at defects, can be used to form visible light emitting porous Si selectively. At present, the size of the structures appears to be limited only by the diameter of the writing ion beam. Thus patterns in the 50 to 200 nm range seem possible.

Recently, electroluminescent devices based on large scale porous Si structures have been reported [9]. The process described in this Letter could facilitate a drastic shrinkage of such device dimensions and hence could be a basis for (or part of) a process leading to extremely high resolution optoelectronic applications.

Additionally, the above findings show that surface lattice defects represent centers of enhanced dissolution, and hence represent the initiation site for pore formation, when conditions are established where Schottky barrier breakdown is the rate-determining step for the surface dissolution reaction.

The authors thank H. G. Champion, J. W. Fraser, and H. J. Labbé for their meticulous help with the experiments and the Swiss National Science Foundation for financial support.

[1] *Light Emission in Silicon,* edited by D. J. Lockwood (Academic, Boston, 1997).
[2] L. T. Canham, Appl. Phys. Lett. **57**, 1046 (1990).
[3] A. G. Cullis and L. T. Canham, Nature (London) **353**, 335 (1991).

[4] V. Lehmann and U. Gösele, Appl. Phys. Lett. **58**, 856 (1991).
[5] *Porous Silicon Science and Technology*, edited by J.-C. Vial and J. Derrier (Springer-Verlag, Berlin, 1995).
[6] J. L. Heinrich, C. L. Curtis, G. M. Credo, K. L. Kavanagh, and M. J. Sailor, Science **255**, 66 (1992).
[7] Special issue [J. Lumin. **57**, 1–358 (1993)].
[8] *Porous Silicon*, edited by Z. C. Feng and R. Tsu (World Scientific, Singapore, 1994).
[9] K. D. Hirschmann, L. Tsybeskov, S. P. Duttagupta, and P. M. Fauchet, Nature (London) **384**, 338 (1996).
[10] S. P. Duttagupta, C. Peng, P. M. Fauchet, S. K. Kurinec, and T. N. Blanton, J. Vac. Sci. Technol. B **13**, 1230 (1995).
[11] V. V. Doan and M. J. Sailor, Science **256**, 1791 (1992).
[12] A. J. Steckl, J. Xu, H. C. Mogul, and S. Mogren, Appl. Phys. Lett. **62**, 1982 (1993).
[13] J. Xu and A. J. Steckl, Appl. Phys. Lett. **65**, 2081 (1994).
[14] J. C. Barbour, D. Dimos, T. R. Guilinger, M. J. Kelly, and S. S. Tsao, Appl. Phys. Lett. **59**, 2088 (1991).
[15] X.-M. Bao and H.-Q. Yang, Appl. Phys. Lett. **63**, 2246 (1993).
[16] P. Schmuki, L. E. Erickson, G. Champion, B. F. Mason, J. W. Fraser, and C. Moessner, Appl. Phys. Lett. **70**, 1305 (1997).
[17] J. F. Ziegler, J. P. Biersack, and U. Littmark, *The Stopping and Range of Ions in Solids* (Pergamon, New York, 1985).
[18] S. M. Sze, *Physics of Semiconductor Devices* (Wiley, New York, 1981).
[19] S. R. Morrison, *Electrochemistry at Semiconductor and Oxidized Metal Electrodes* (Plenum, New York, 1980).
[20] A. G. Cullis, L. T. Canham, and P. D. J. Calcott, J. Appl. Phys. **82**, 909 (1997).